

Tunable and Switchable Coupling Between Two Superconducting Resonators

A. Baust,^{1,2,3,*} E. Hoffmann,^{1,2,†} M. Haerberlein,^{1,2} M. J. Schwarz,^{1,2,3} P. Eder,^{1,2,3} E. P. Menzel,^{1,2} K. Fedorov,^{1,2} J. Goetz,^{1,2} F. Wulschner,^{1,2} E. Xie,^{1,2} L. Zhong,^{1,2,3} F. Quijandria,⁴ B. Peropadre,^{5,6} D. Zueco,^{4,7} J.-J. Garcia Ripoll,⁵ E. Solano,^{8,9} F. Deppe,^{1,2,3} A. Marx,¹ and R. Gross^{1,2,3,‡}

¹Walther-Meißner-Institut, Bayerische Akademie der Wissenschaften, D-85748 Garching, Germany

²Physik-Department, Technische Universität München, D-85748 Garching, Germany

³Nanosystems Initiative Munich (NIM), Schellingstraße 4, 80799 München, Germany

⁴Instituto de Ciencia de Materiales de Aragón and Departamento de Física de la Materia Condensada, CSIC-Universidad de Zaragoza, 50009 Zaragoza, Spain

⁵Instituto de Física Fundamental, IFF-CSIC, Calle Serrano 113b, Madrid E-28006, Spain

⁶Department of Chemistry and Chemical Biology,

Harvard University, Cambridge, Massachusetts 02138, United States

⁷Fundación ARAID, Paseo María Agustín 36, 50004 Zaragoza, Spain

⁸Department of Physical Chemistry, University of the Basque Country UPV/EHU, Apartado 644, E-48080 Bilbao, Spain

⁹IKERBASQUE, Basque Foundation for Science, Alameda Urquijo 36, 48011 Bilbao, Spain

(Dated: December 6, 2024)

We realize a device allowing for tunable and switchable coupling between two superconducting resonators mediated by an artificial atom. For the latter, we utilize a persistent current flux qubit. We characterize the tunable and switchable coupling in frequency and time domain and find that the coupling between the relevant modes can be varied in a controlled way. Specifically, the coupling can be tuned by adjusting the flux through the qubit loop or by saturating the qubit. Our time domain measurements allow us to find parameter regimes for optimal switch performance with respect to qubit drive power and the dynamic range of the resonator input power.

PACS numbers: 03.67.Lx, 85.25.Am, 85.25.Cp

Circuit quantum electrodynamics (QED) [1] has become a well-established platform for the investigation of light-matter interaction [2], quantum information processing and recently quantum simulation [3–5]. One of the most important advantages in using superconducting circuits for these purposes is the large coupling strength between the main building blocks, namely superconducting quantum bits and microwave resonators. However, to realize quantum gates and quantum information and simulation protocols, the coupling between the individual circuit elements needs to be tunable *in situ*. This can be realized in at least two ways. One way is to decouple two circuits by detuning them in frequency, for example by using the frequency tunability of superconducting qubits. With this technique, systems with up to five qubits and up to five microwave resonators were studied [5–7], entangled quantum states were created [8–10] and quantum teleportation [11] and quantum computing protocols were demonstrated [12–14]. Alternatively, the coupling between two circuit QED building blocks can be mediated by additional coupling circuits. Examples for coupling circuits include single Josephson junctions [15, 16], SQUIDs [17–19] or qubits [20, 21] which were used to realize tunable coupling between qubits, resonators and transmission lines. Furthermore, new types of qubits were introduced featuring intrinsic tunability of the coupling to microwave resonators [22–24]. In this work, we report on tunable and switchable coupling between two superconducting transmission line resonators mediated by a superconducting flux qubit.

Our setup, which we call quantum switch according to Refs. [25, 26], is in a way dual to the usage of a resonator as quantum bus between two qubits [27, 28]. We show that the coupling between the two resonators can be controlled by tuning the magnetic flux applied to the qubit loop or by driving the qubit. We perform time domain measurements to find the parameter regimes for optimal sample performance.

The quantum switch sample comprises two coplanar stripline resonators, A and B, with fundamental mode frequencies $\omega_R/2\pi = 4.896$ GHz as shown in Fig. 1(a)-(c) and a superconducting flux qubit or artificial atom. The resonators are fabricated in Nb technology on a thermally oxidized Si substrate. The linewidths of the fundamental modes of both resonators for the qubit being far detuned were determined as $\gamma_A/2\pi = 2.3$ MHz and $\gamma_B/2\pi = 0.5$ MHz. The detuning between the two resonators is found to be small and is therefore neglected. An artificial atom is coupled galvanically to the signal lines of both resonators at the position of the current antinodes of their fundamental modes, cf. Fig. 1(c)-(e). In our case, this artificial atom is a flux qubit consisting of a superconducting Al loop with three Josephson junctions where one of the junctions is smaller by a factor $\alpha = 0.7$. For the qubit we determine an energy gap $\Delta/\hbar = 3.52$ GHz and a persistent current $I_p = 477$ nA. The coupling between the qubit and each resonator is $g/2\pi = 110$ MHz. The qubit parameters determined by two-tone spectroscopy can be quantitatively described

by taking into account the galvanic coupling of the qubit to the resonators in our quantum switch setup.

The effective Hamiltonian for the qubit coupled to the fundamental modes of the two resonators is [25, 26]

$$\hat{H}_{\text{eff}} = \hbar \frac{\omega_Q}{2} \hat{\sigma}_z + \hbar (\omega_R + g_{\text{dyn}} \hat{\sigma}_z) (\hat{a}^\dagger \hat{a} + \hat{b}^\dagger \hat{b}) + \hbar (g_{\text{AB}} + g_{\text{dyn}} \hat{\sigma}_z) (\hat{a}^\dagger \hat{b} + \hat{a} \hat{b}^\dagger). \quad (1)$$

Here, $\omega_Q = \sqrt{\epsilon^2 + \Delta^2}/\hbar$ is the qubit transition frequency with the energy bias $\epsilon(\Phi_{\text{ext}}) = 2I_p(\Phi_{\text{ext}} - \frac{1}{2}\Phi_0)$, Φ_0 is the flux quantum, and Φ_{ext} is the external magnetic flux threading the qubit loop. The flux degeneracy point $\Phi_{\text{ext}} = \frac{\Phi_0}{2}$ corresponds to $\omega_Q = \Delta$. Furthermore, we denote the annihilation (creation) operators for the two resonators A and B as \hat{a} and \hat{b} (\hat{a}^\dagger and \hat{b}^\dagger). The coupling between the two resonators is mediated by two mechanisms. In addition to the geometrical coupling $g_{\text{AB}}/2\pi = 8.4$ MHz between the two resonators there is the second-order *dynamic coupling*

$$g_{\text{dyn}} = \frac{(g \sin \theta)^2}{|\omega_Q - \omega_R|} + \frac{(g \sin \theta)^2}{\omega_Q + \omega_R}$$

which can be tuned via Φ_{ext} since both the mixing angle $\tan \theta = \Delta/\epsilon$ and the qubit transition frequency ω_Q are flux dependent. We gain further insight by considering the normal modes of the coupled resonators $\hat{c}_\pm = \frac{1}{\sqrt{2}}(\hat{a} \pm \hat{b})$ and $\hat{c}_\pm^\dagger = \frac{1}{\sqrt{2}}(\hat{a}^\dagger \pm \hat{b}^\dagger)$, which allow us to rewrite the Hamiltonian of Eq. (1) to

$$\hat{H}_{\text{eff}} = \hbar \frac{\omega_Q}{2} \hat{\sigma}_z + \hbar \omega_R (\hat{c}_+^\dagger \hat{c}_+ + \hat{c}_-^\dagger \hat{c}_-) + \hbar g_{\text{AB}} (\hat{c}_+^\dagger \hat{c}_+ - \hat{c}_-^\dagger \hat{c}_-) + 2\hbar g_{\text{dyn}} \hat{\sigma}_z (\hat{c}_+^\dagger \hat{c}_+) \quad (2)$$

The modes \hat{c}_- and \hat{c}_+ correspond to in-phase and out-of-phase oscillating currents in the two resonators, respectively. As only the out-of-phase oscillating mode generates a magnetic field at the position of the qubit, only this mode couples to the qubit.

For our measurements, we mount the sample inside a gold-plated copper box to the base temperature stage of a dilution refrigerator. The sample temperature is stabilized at 45 mK. As shown in Fig. 1(f) one port of each resonator is connected to a highly attenuated input line while the respective second port is connected to an output line featuring cryogenic and room temperature amplifiers. In this way, we can measure the transmission through the individual resonators (referred to as a 'through'-measurement) but also the transmission from the input of one resonator to the output of the second resonator ('cross'-measurement). A superconducting solenoid is mounted on top of the sample package in order to apply magnetic flux to the qubit loop.

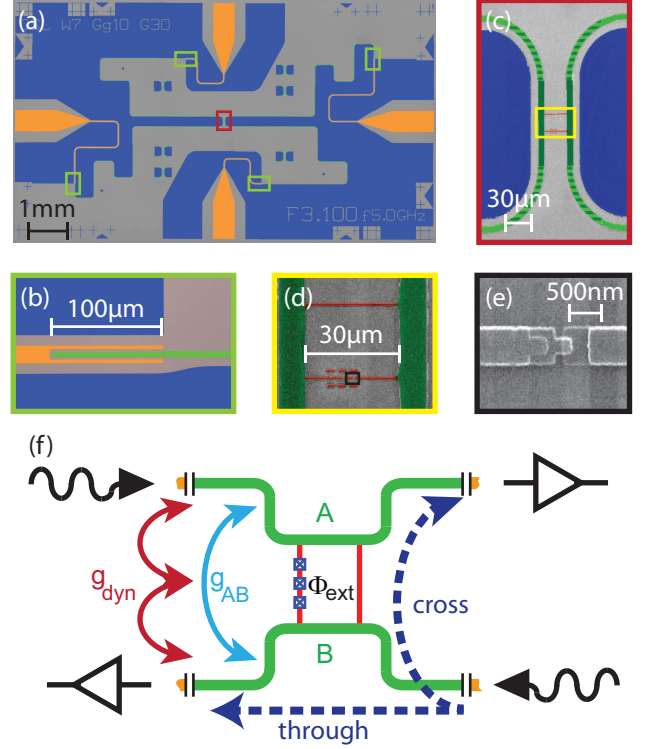


FIG. 1. (color online) (a) False-color image of the quantum switch sample. Nb ground planes are shown in blue and feed lines in orange. The resonator signal lines reside along the ground plane edges. (b) Coupling capacitor defining the resonators. (c) Resonator coupling area with signal lines (green) and flux qubit (red). Light/dark green stripes highlight Nb-Al overlap areas. (d) Flux qubit galvanically coupled to both resonators. (e) Al/AIO_x/Al Josephson junction fabricated using shadow evaporation. (f) Working principle of the quantum switch and measurement setup.

To determine the relevant sample parameters and to characterize the switch properties, we first measure the transmission through the quantum switch sample with a vector network analyzer depending on the applied magnetic flux Φ_{ext} . Fig. 2(a) shows the results of a 'through'-measurement whereas Fig. 2(b) represents a 'cross'-measurement. For both measurements, the input signal is applied to the same port and the qubit remains in the ground state. The input power is chosen such that the population of both resonators is approximately one photon on average. We observe two modes as expected for coupled resonators, where the splitting far away from the qubit degeneracy point is $2g_{\text{AB}}$. If the flux is tuned towards the degeneracy point, the frequency of the lower mode stays constant while the frequency of the upper mode is shifted to lower frequencies as expected from Eq. (2).

In this way, the flux can be tuned such that the frequency of the upper mode matches the frequency of the lower mode. We refer to these points as the *switch setting*

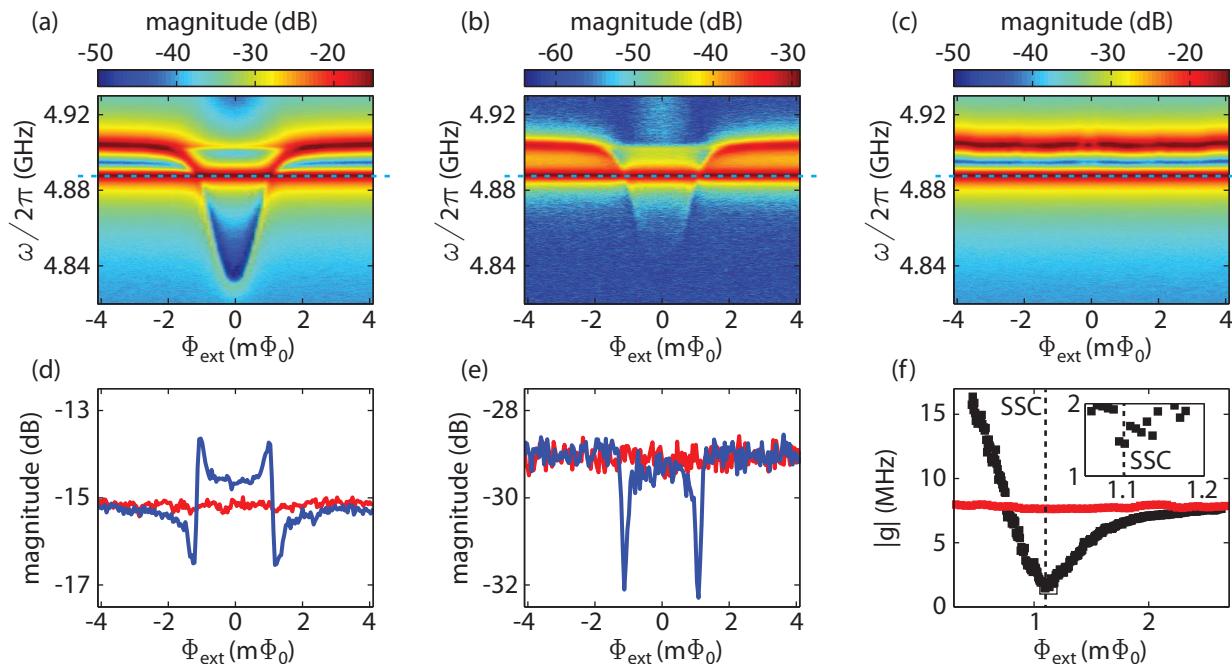


FIG. 2. (color online) (a) Transmission through one resonator depending on the applied magnetic flux with the qubit in ground state. (b) ‘Cross’ measurement, qubit in ground state. (c) ‘Through’ measurement, qubit driven with strong excitation signal. (d) ‘Through’ measurement, transmission at the frequency of the lower mode at 4.888 GHz [dashed lines in (a) and (c)] with qubit in ground state (blue line) and saturated qubit (red line). (e) Same as (d) for the ‘cross’ measurement. (f) Magnitude of the total coupling between the resonators extracted from a ‘through’ measurement near the switch setting condition. Black: qubit in ground state. Red: saturated qubit. Inset: Measurement with increased flux resolution around switch setting condition (SSC).

conditions where the geometrical coupling is fully compensated by the dynamical coupling. Consequently, the two resonators are expected to be decoupled from each other if the switch setting condition is fulfilled. In order to find the minimum value of the coupling for our device, we fit the mode spectrum shown in Fig. 2(a) using input-output theory [29, 30] and analyze the coupling depending on the magnetic flux. Results are shown in Fig. 2(f). At the switch setting condition, the coupling is reduced to $|g_{\min}/2\pi| \lesssim 1.5$ MHz. Here, our analysis is limited by the decay rates of the resonators. Compared to the coupling far off the degeneracy point, the coupling at the switch setting condition is reduced by a factor of 5.5.

So far, we have investigated how to tune the coupling via the magnetic flux applied to the qubit loop. Next, we show that the coupling is also controlled by the qubit population as expected from Eq. (2). To this end, we record the resonator transmission while driving the qubit with a strong excitation signal applied through the input port of the other resonator. This results in equal probabilities to find the qubit in the ground and excited state, yielding $\langle \hat{\sigma}_z \rangle = \text{Tr}[\rho_M \hat{\sigma}_z] = 0$ where $\rho_M = \frac{1}{2}(|g\rangle\langle g| + |e\rangle\langle e|)$. As expected from Eq. (1) we observe that the coupling between the two resonators is then given by g_{AB} independently of the applied flux, see Fig. 2(c) and Fig. 2(f). To analyze the interplay of flux- and qubit state dependence in more detail, we show

the transmission at the frequency of the lower mode at $\omega/2\pi = 4.888$ GHz in Fig. 2(d) and Fig. 2(e). For the qubit in the ground state, we observe increased transmission for the ‘through’-measurement at the switch setting conditions compared to flux values not matching a switch setting condition or compared to the qubit being driven. This is in agreement with our expectation that, when turning off the coupling, the signal incident on one resonator cannot cross over to the other one. Consistently, we observe reduced transmission at the switch setting condition in the ‘cross’ measurement shown in Fig. 2(e). Two dips are visible in the through transmission [Fig. 2(d)], when the qubit is in the ground state. They originate from the differences in the linewidths and also from a possible small detuning between the two resonators. Furthermore, we note that the galvanic coupling of the qubit to both resonators results in the existence of additional resonant modes. They are not discussed here in detail since they have no influence on the qualitative behaviour of the quantum switch. Due to the highly symmetric design of our sample, one of these additional modes is frequency degenerate with the out-of-phase quantum switch mode when the qubit is far detuned from the degeneracy point [see Fig. 2(a) and Fig. 2(b)].

Next, we conduct time domain experiments making the switchable coupling directly observable. To this end,

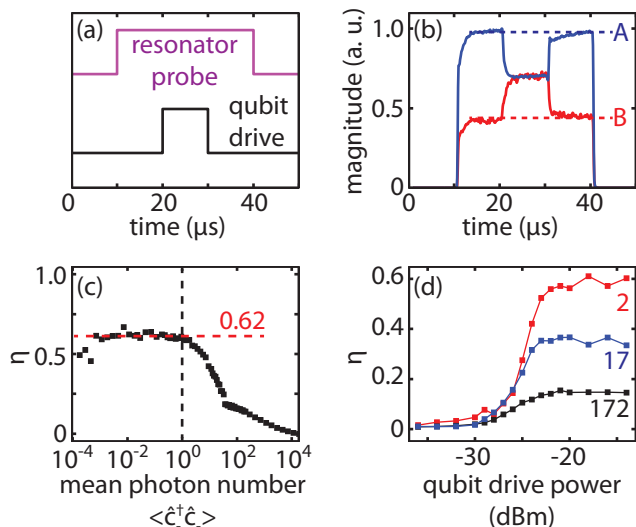


FIG. 3. (color online) (a) Pulse pattern for the time-domain probe of the quantum switch. (b) Typical measured time traces of the output signals of the two resonators. Blue: 'through' transmission measurement. red: 'cross' transmission measurement. The power is referred to the inside of the resonators, i.e. they are scaled such that they are equal when the coupling is 'on'. (c) Switching efficiency η as a function of the mean resonator population. (d) Switching efficiency as a function of the qubit drive power (referenced to signal generator output) measured for three different resonator populations.

we set the flux bias corresponding to the switch setting condition and apply a microwave probe pulse (length $\tau_{\text{res}} = 30 \mu\text{s}$) to one of the resonators at the frequency $\omega_{\text{res}}/2\pi = 4.888 \text{ GHz}$ of the lower (\hat{c}_-) mode. In addition, a strong $10 \mu\text{s}$ long microwave driving pulse switches the coupling between the resonators on for a period of $10 \mu\text{s}$ as shown in Fig. 3(a). The output signals of both resonators are detected in a time-resolved way using an FPGA-enhanced A/D-converter. A typical pair of time traces is shown in Fig. 3(b). After switching on the qubit drive, the output signal level of the resonator where the drive pulse is applied decreases, whereas it increases for the other resonator. This result represents a direct experimental evidence for the expected switching behaviour because it implies that the transfer of energy from one into another resonator can be controlled via the qubit. However, for an ideal quantum switch, one would expect that at the switch setting condition the output signal level for the 'cross'-measurement is zero when the qubit is in the ground state, even if the probe pulse is on. Nevertheless, in our case a finite output power can be observed. We attribute this to the presence of the frequency degenerate additional mode as discussed above, cf. Fig. 2(a) and Fig. 2(b). To quantify the switch performance, we define the switching efficiency $\eta \equiv 1 - \frac{B}{A}$. As indicated in Fig. 3(b), A denotes the output power level of the 'through' resonator and B is the output power level

of the 'cross' resonator when the qubit is in the ground state. We assume that when the coupling between the resonators is switched on, the mean photon population is equal in both resonators as predicted by input-output theory (because $g_{AB} > \gamma_{A,B}$) and that for both resonators the output power is proportional to the respective resonator population. Hence, the ratio of the mean photon population of the 'cross' and the 'through' resonator is given by $1 - \eta$.

Next, we analyze η as a function of mean number of photons (calibrated via dispersive shift of the qubit; data not shown) in the \hat{c}_- -mode. The results are shown in Fig. 3(c). For low photon numbers we find a switching efficiency of $\eta \approx 0.62$ limited by the additional modes which represent an additional coupling channel between the resonators which cannot be tuned like the quantum switch mode. Above approximately 1 photon, η starts to decrease and vanishes for photon numbers exceeding 10^4 . This behaviour is in agreement with the disappearance of the Jaynes-Cummings-doublet due to a quantum-to-classical transition observed in a transmon-resonator system [31]. Finally, we analyze the switching efficiency depending on the qubit drive power, cf. Fig. 3(d). For high drive power values, η is maximum, whereas it decreases when the drive power is reduced and the qubit is no longer fully saturated. For very low drive powers, the switching efficiency drops to zero. The critical drive power between the regimes is independent of the resonator population.

In conclusion, we present a device allowing to tune the coupling between two coplanar stripline resonators via a flux qubit coupled to both of them. We characterize the individual constituents and the switching behaviour by means of spectroscopy and perform a quantitative analysis of the switching performance using a time domain experiment. We find a maximum switching efficiency of 62%. For our particular sample, the switch performance is limited by additional modes originating from the galvanic qubit-resonator coupling and the highly symmetric layout of the sample. However, these additional modes are not relevant for the analysis presented in this paper. We expect that the limitations caused by these additional modes can be overcome by placing the qubit slightly off the centers of the resonators and thus separate all additional modes in frequency from the relevant quantum switch modes. Such improved designs are promising candidates for applications in future quantum information processing setups where the quantum switch can be used for the controlled transfer of excitations between a fast bus resonator, to which additional qubits can be coupled, and a long-lived storage resonator serving as quantum memory. Furthermore, the quantum switch may become a key element in quantum simulation architectures such as chains or networks of superconducting nonlinear resonators for the simulation of the Bose-Hubbard-Hamiltonian [32].

This work is supported by the German Research Foundation through SFB 631, EU projects CCQED, PROMISCE and SQALEQIT, Spanish Mineco projects FIS2012-33022 and FIS2012-36673-C03-02, UPV/EHU UFI 11/55 and Basque Government IT472-10.

* Alexander.Baust@wmi.badw-muenchen.de

† A.B. and E.H. contributed equally to this work.

‡ Rudolf.Gross@wmi.badw-muenchen.de

- [1] A. Wallraff, D. I. Schuster, A. Blais, L. Frunzio, R.-S. Huang, J. Majer, S. Kumar, S. M. Girvin, and R. J. Schoelkopf, *Nature* **431**, 162 (2004).
- [2] T. Niemczyk, F. Deppe, H. Huebl, E. P. Menzel, F. Hocke, M. J. Schwarz, J. J. Garcia-Ripoll, D. Zueco, T. Hummer, E. Solano, A. Marx, and R. Gross, *Nat Phys* **6**, 772 (2010).
- [3] A. A. Houck, H. E. Türeci, and J. Koch, *Nat Phys* **8**, 292 (2012).
- [4] J. Raftery, D. Sadri, S. Schmidt, H. E. Türeci, and A. A. Houck, (2013), [arXiv:1312.2963](https://arxiv.org/abs/1312.2963).
- [5] Y. Chen, P. Roushan, D. Sank, C. Neill, E. Lucero, M. Mariantoni, R. Barends, B. Chiaro, J. Kelly, A. Megrant, J. Y. Mutus, P. J. J. O'Malley, A. Vainsencher, J. Wenner, T. C. White, Y. Yin, A. N. Cleland, and J. M. Martinis, (2014), [arXiv:1403.6808](https://arxiv.org/abs/1403.6808).
- [6] E. Lucero, R. Barends, Y. Chen, J. Kelly, M. Mariantoni, A. Megrant, P. O'Malley, D. Sank, A. Vainsencher, J. Wenner, T. White, Y. Yin, A. N. Cleland, and J. M. Martinis, *Nat Phys* **8**, 719 (2012).
- [7] R. Barends, J. Kelly, A. Megrant, A. Veitia, D. Sank, E. Jeffrey, T. C. White, J. Mutus, A. G. Fowler, B. Campbell, Y. Chen, Z. Chen, B. Chiaro, A. Dunsworth, C. Neill, P. O'Malley, P. Roushan, A. Vainsencher, J. Wenner, A. N. Korotkov, A. N. Cleland, and J. M. Martinis, *Nature* **508**, 500 (2014).
- [8] C. Eichler, C. Lang, J. M. Fink, J. Govenius, S. Filipp, and A. Wallraff, *Phys. Rev. Lett.* **109**, 240501 (2012).
- [9] O.-P. Saira, J. P. Groen, J. Cramer, M. Meretska, G. de Lange, and L. DiCarlo, *Phys. Rev. Lett.* **112**, 070502 (2014).
- [10] L. DiCarlo, M. D. Reed, L. Sun, B. R. Johnson, J. M. Chow, J. M. Gambetta, L. Frunzio, S. M. Girvin, M. H. Devoret, and R. J. Schoelkopf, *Nature* **467**, 574 (2010).
- [11] L. Steffen, Y. Salathe, M. Oppliger, P. Kurpiers, M. Baur, C. Lang, C. Eichler, G. Puebla-Hellmann, A. Fedorov, and A. Wallraff, *Nature* **500**, 319 (2013).
- [12] A. Dewes, R. Lauro, F. R. Ong, V. Schmitt, P. Milman, P. Bertet, D. Vion, and D. Esteve, *Phys. Rev. B* **85**, 140503 (2012).
- [13] A. Dewes, F. R. Ong, V. Schmitt, R. Lauro, N. Boulant, P. Bertet, D. Vion, and D. Esteve, *Phys. Rev. Lett.* **108**, 057002 (2012).
- [14] M. D. Reed, L. DiCarlo, S. E. Nigg, L. Sun, L. Frunzio, S. M. Girvin, and R. J. Schoelkopf, *Nature* **482**, 382 (2012).
- [15] Y. Chen, C. Neill, P. Roushan, N. Leung, M. Fang, R. Barends, J. Kelly, B. Campbell, Z. Chen, B. Chiaro, A. Dunsworth, E. Jeffrey, A. Megrant, J. Y. Mutus, P. J. J. O'Malley, C. M. Quintana, D. Sank, A. Vainsencher, J. Wenner, T. C. White, M. R. Geller, A. N. Cleland, and J. M. Martinis, (2014), [arXiv:1402.7367](https://arxiv.org/abs/1402.7367).
- [16] R. C. Bialczak, M. Ansmann, M. Hofheinz, M. Lenander, E. Lucero, M. Neeley, A. D. O'Connell, D. Sank, H. Wang, M. Weides, J. Wenner, T. Yamamoto, A. N. Cleland, and J. M. Martinis, *Phys. Rev. Lett.* **106**, 060501 (2011).
- [17] T. Hime, P. A. Reichardt, B. L. T. Plourde, T. L. Robertson, C.-E. Wu, A. V. Ustinov, and J. Clarke, *Science* **314**, 1427 (2006).
- [18] Y. Yin, Y. Chen, D. Sank, P. J. J. O'Malley, T. C. White, R. Barends, J. Kelly, E. Lucero, M. Mariantoni, A. Megrant, C. Neill, A. Vainsencher, J. Wenner, A. N. Korotkov, A. N. Cleland, and J. M. Martinis, *Phys. Rev. Lett.* **110**, 107001 (2013).
- [19] B. Peropadre, D. Zueco, F. Wulschner, F. Deppe, A. Marx, R. Gross, and J. J. Garcia-Ripoll, *Phys. Rev. B* **87**, 134504 (2013).
- [20] A. O. Niskanen, K. Harrabi, F. Yoshihara, Y. Nakamura, S. Lloyd, and J. S. Tsai, *Science* **316**, 723 (2007).
- [21] I.-C. Hoi, A. F. Kockum, T. Palomaki, T. M. Stace, B. Fan, L. Tornberg, S. R. Sathyamoorthy, G. Johansson, P. Delsing, and C. M. Wilson, *Phys. Rev. Lett.* **111**, 053601 (2013).
- [22] A. J. Hoffman, S. J. Srinivasan, J. M. Gambetta, and A. A. Houck, *Phys. Rev. B* **84**, 184515 (2011).
- [23] S. J. Srinivasan, A. J. Hoffman, J. M. Gambetta, and A. A. Houck, *Phys. Rev. Lett.* **106**, 083601 (2011).
- [24] J. M. Gambetta, A. A. Houck, and A. Blais, *Phys. Rev. Lett.* **106**, 030502 (2011).
- [25] M. Mariantoni, F. Deppe, A. Marx, R. Gross, F. K. Wilhelm, and E. Solano, *Phys. Rev. B* **78**, 104508 (2008).
- [26] G. M. Reuther, D. Zueco, F. Deppe, E. Hoffmann, E. P. Menzel, T. Weissl, M. Mariantoni, S. Kohler, A. Marx, E. Solano, R. Gross, and P. Hänggi, *Phys. Rev. B* **81**, 144510 (2010).
- [27] M. A. Sillanpää, J. I. Park, and R. W. Simmonds, *Nature* **449**, 438 (2007).
- [28] J. Majer, J. M. Chow, J. M. Gambetta, J. Koch, B. R. Johnson, J. A. Schreier, L. Frunzio, D. I. Schuster, A. A. Houck, A. Wallraff, A. Blais, M. H. Devoret, S. M. Girvin, and R. J. Schoelkopf, *Nature* **449**, 443 (2007).
- [29] D. Walls and G. Milburn, *Quantum Optics* (Springer, 2008).
- [30] C. Sames, H. Chibani, C. Hamsen, P. A. Altin, T. Wilk, and G. Rempe, *Phys. Rev. Lett.* **112**, 043601 (2014).
- [31] J. M. Fink, L. Steffen, P. Studer, L. S. Bishop, M. Baur, R. Bianchetti, D. Bozyigit, C. Lang, S. Filipp, P. J. Leek, and A. Wallraff, *Phys. Rev. Lett.* **105**, 163601 (2010).
- [32] M. Leib, F. Deppe, A. Marx, R. Gross, and M. J. Hartmann, *New Journal of Physics* **14**, 075024 (2012).